The Ground State Estimation by Global Optimization of an Effective Potential. Application to Binary para-H-2/ortho-D-2 Molecular Clusters

ARTICLE *in* THE JOURNAL OF PHYSICAL CHEMISTRY A · SEPTEMBER 2010

Impact Factor: 2.69 · DOI: 10.1021/jp102898b · Source: PubMed

2 AUTHORS, INCLUDING:

Jason Deckman
University of California, Irvine
10 PUBLICATIONS **58** CITATIONS

The Ground State Estimation by Global Optimization of an Effective Potential. Application to Binary *para*-H_2/*ortho*-D_2 Molecular Clusters†

Jason Deckman and Vladimir A. Mandelshtam*

Chemistry Department, University of California at Irvine, Irvine, California 92697, USA

Received: March 31, 2010; Revised Manuscript Received: May 26, 2010

It is demonstrated how the problem of ground state estimation of an *n*-body system can be recast as the less demanding problem of finding the global minimum of an effective potential in the 3*n*-dimensional coordinate space. The latter emerges when the solution of the imaginary-time Schrödinger equation is approximated by a variational Gaussian wavepacket (VGW). The VGW becomes stationary in the infinite-imaginary-time limit. Such a stationary solution is not only exact for a harmonic potential, but it also provides a good approximation for a quantum state that is still localized in one of the basins of attraction, when, for example, the harmonic approximation may fail. The landscape of the effective potential is favorable for its global optimization, and is particularly suitable for optimization by GMIN, an open source program designed for global optimization using the basin-hopping algorithm. Consequently, the methodology is applied within GMIN to estimate the ground state structures of several binary *para*-H_2/*ortho*-D_2 molecular clusters. The results are generally consistent with the previous observations for homogeneous *para*-H_2 and *ortho*-D_2 clusters, as well as for smaller binary clusters.

Introduction

Theoretical studies of atomic and molecular clusters continue to comprise an active area of research, owing to their applications in areas ranging from global optimization[1,2] to nanotechnology. With regard to the former, their simulation serves as a test ground for the benchmarking of new algorithms, and for the latter, finding, for example, the minimum energy configurations reveals what structures may be encountered experimentally.

A well researched problem is the characterization of the potential energy surface (PES). With increasing cluster size the number of low energy local minima grows so dramatically[3] that their adequate sampling (e.g., in order to find the global energy minimum) is often beyond the limit of computing power and we can only estimate what the global minimum configuration may be and what the low energy motifs at finite temperatures are.

Monte Carlo (MC) methods are commonly employed in various contexts to sample the configuration space. To adequately characterize the PES, the numerous local minima that pertain to the configurational isomers of a cluster need to be accounted for. Algorithms, such as replica exchange Monte Carlo (REMC),[4] basin-hopping,[5,6] etc., significantly assist in this process. An open source program, GMIN, for finding global minima and calculating thermodynamic properties of classical many-body systems using basin-sampling exists.[7] However, it does not take into account the quantum effects, which may be significant for a broad range of atomic and molecular systems.

In addition to the classical sampling problems, accounting for quantum effects further adds to the complexity. The path integral Monte Carlo (PIMC) methods (see, e.g., ref 8) provide in principle exact results for equilibrium properties at finite temperatures, and, in particular, for the ground state, when the $T \rightarrow 0$ limit is employed. Contrary to one's intuition, strong quantum effects may simplify the problem, for example, by smoothing the effective PES and therefore reducing its complexity. This is probably the case for helium systems. However, a weakly quantum system (e.g., considering neon), that is, when the quantum delocalization is not sufficiently strong, is still very complex (e.g., in terms of the effective PES). Thus, characterizing a weakly quantum system with a complex PES must be at least as difficult as that for the purely classical system, which, again, if feasible at all, often requires a substantial numerical effort.

On the other hand, for a weakly quantum system, the ground state wave function is usually well localized in one of the local minima (or basins of attraction) of the PES and as such can often be approximated by a simple shape (e.g., a Gaussian). For example, ref 11 presents an analysis based on the harmonic approximation (HA)[12] of the ground state structures of certain weakly quantum Lennard−Jones (LJ) clusters corresponding to the rare gas atomic clusters. Although the HA is straightforward to implement and it may be adequate for nearly classical cases, such as xenon or argon clusters, in a more quantum regime, for example, neon, the predictions of the HA are very crude. A more accurate method, while computationally still feasible, is the variational Gaussian wavepacket (VGW) approximation.[9,10] In ref 13 it was implemented for estimating the ground states of LJ_n clusters as a function of their size *n* and the de Boer quantum delocalization length[14] $\Lambda = (\hbar/\sqrt{m\varepsilon})/\sigma$, where the LJ potential is defined by

$$V(r_{ij}) = 4\varepsilon\left[\left(\frac{\sigma}{r_{ij}}\right)^{12} - \left(\frac{\sigma}{r_{ij}}\right)^{6}\right] \quad (1)$$

The resulting $n - \Lambda$ phase diagram, revealing the structural motifs of the LJ clusters, can now serve as a reference for similar studies of van der Waals clusters, for which the pair interactions can be mapped to the LJ potential.

† Part of the "Reinhard Schinke Festschrift".

* To whom correspondence should be addressed. E-mail: mandelsh@uci.edu.

10.1021/jp102898b
Published on Web 06/11/2010

Interestingly, the VGW approximation leads naturally to the introduction of an effective PES, which can, in turn, be utilized within the GMIN package. That is, when extended to a global optimization of the effective PES, GMIN can be used for the ground state calculations! Consequently, in the present work we incorporated the VGW method into GMIN and applied it to estimate the ground state structures of several composite clusters of p-H_2/o-D_2.

Both homogeneous and binary p-H_2/o-D_2 clusters have already been studied in a number of publications using the PIMC-based approaches (see for examples refs 15−22). So, we can relate our results to the latter.

In simulations of classical LJ clusters, it is demonstrated that species with a shallower pair-interaction well depth (ε) and larger radius (σ) reside on the outer shell of the cluster.[23−25] The analog of this from quantum simulations of p-H_2/o-D_2 clusters is for the heavier o-D_2 to occupy the core while the lighter p-H_2 lie on the surface.[17,19,20] Thus, in the current study we should expect to observe ground state structures with o-D_2 comprising the core and p-H_2 occupying the surface, with perhaps a higher order relative to a cluster of pure p-H_2. Additionally, the introduction of an impurity into homogeneous p-H_2 clusters has been reported to have a "freezing" effect, whereby the inherently liquid-like state of these pure clusters becomes more ordered in the presence of a different species.[19,20]

It is worth noting that for each local minimum of $(H_2)_n$ the number of distinct local minima of the binary cluster $(H_2)_{n-k}(D_2)_k$ is estimated by $(n!)/(k!(n-k)!)$ (the spatial symmetries reduce this number, but only by the order of the corresponding point group, which is insignificant), that is, characterizing all the relevant configurations becomes quickly unfeasible at relatively small values of n and k. Therefore, we can only hope that the low energy configurations found in this study provide an adequate qualitative description of these systems.

Estimation of the Ground State by VGW

Given n-particle system, the Hamiltonian can be written as

$$\hat{H} = -\frac{\hbar^2}{2}\nabla^T\mathbf{M}^{-1}\nabla + U(\mathbf{r}) \tag{2}$$

with diagonal mass matrix $\mathbf{M} = \mathrm{diag}(m_i)$, assuming Cartesian coordinates. By $\mathbf{r} := (\mathbf{r}_1, ...,\mathbf{r}_n)^T$, we define a $3n$-vector containing the particle coordinates. $\nabla := (\nabla_1, ...,\nabla_n)^T$ represents the gradient. Within the VGW approximation the wave functions are approximated by Gaussians of the form

$$\Psi = \exp\left[-\frac{1}{2}(\mathbf{r}-\mathbf{q})^T\mathbf{G}^{-1}(\mathbf{r}-\mathbf{q}) + \gamma\right] \tag{3}$$

with the following variational parameters: the Gaussian width $\mathbf{G}$ (a $3n \times 3n$ real symmetric, positive definite matrix), the Gaussian center $\mathbf{q}$ (a real $3n$-vector), and a scaling factor γ. The Gaussians are propagated in imaginary time τ according to the Bloch equation

$$|\mathbf{q}_0;\tau\rangle = \mathrm{e}^{-\tau\hat{H}}|\mathbf{q}_0;0\rangle \tag{4}$$

The propagation is carried out by solving the system of coupled ordinary differential equations for the Gaussian parameters, $\mathbf{q}_\tau$, $\mathbf{g}_\tau$, and γ_τ,

$$\begin{cases} \dfrac{\mathrm{d}}{\mathrm{d}\tau}\mathbf{G}_\tau = -\mathbf{G}_\tau\langle\nabla\nabla^{\mathrm{T}}U\rangle_\psi\mathbf{G}_\tau + \hbar^2\mathbf{M}^{-1} \\ \dfrac{\mathrm{d}}{\mathrm{d}\tau}\mathbf{q}_\tau = -\mathbf{G}_\tau\langle\nabla U\rangle_\psi \\ \dfrac{\mathrm{d}}{\mathrm{d}\tau}\gamma_\tau = -\dfrac{1}{4}\mathrm{Tr}(\langle\nabla\nabla^{\mathrm{T}}U\rangle_\psi\mathbf{G}_\tau) + \langle U\rangle_\psi \end{cases} \tag{5}$$

with initial conditions

$$\begin{aligned} \mathbf{q}_{\tau_0} &= \mathbf{q}_0, \\ \mathbf{G}_{\tau_0} &= \tau_0\hbar^2\mathbf{M}^{-1} \\ \gamma_{\tau_0} &= -\tau_0 U(\mathbf{q}_0) \end{aligned} \tag{6}$$

which are defined for a sufficiently small but otherwise arbitrary value of τ_0.

In eq 5, $\langle U\rangle_\Psi$ represents the averaged (over the Gaussian wavepacket Ψ) potential, $\langle\nabla U\rangle_\Psi$, the averaged force and $\langle\nabla\nabla^{\mathrm{T}}U\rangle_\Psi$, the averaged Hessian:

$$\begin{aligned} \langle U\rangle_\psi &:= \langle\psi|U|\psi\rangle\langle\psi|\psi\rangle^{-1} \\ \langle\nabla U\rangle_\psi &:= \langle\psi|\nabla U|\psi\rangle\langle\psi|\psi\rangle^{-1} \\ \langle\nabla\nabla^{\mathrm{T}}U\rangle_\psi &:= \langle\psi|\nabla\nabla^{\mathrm{T}}U|\psi\rangle\langle\psi|\psi\rangle^{-1} \end{aligned} \tag{7}$$

(For more details see refs 9, 10, and 13)

For each initial configuration $\mathbf{q}_0$ in the $\tau \rightarrow \infty$ limit the solution $|\mathbf{q}_0, \tau\rangle$ becomes stationary with the total number of distinct stationary solutions defined roughly by the total number of local minima of the classical PES $U(\mathbf{r})$. That is, there is at most one stationary solution associated with each minimum (the VGWs may be delocalized over several local minima though).

A wave function Ψ can be characterized using various spatial correlation functions, such as the radial pair correlation function

$$p(r) = \sum_{i>j}\langle\delta(r_{ij} - r)\rangle_\Psi \tag{8}$$

with

$$\langle\delta(r_{ij} - r)\rangle_\psi = \langle\psi|\delta(\mathrm{r_{ij}} - r)|\psi\rangle\langle\psi|\psi\rangle^{-1}$$

For a Gaussain wavepacket $\Psi = |\mathbf{q}_0, \tau\rangle$, the latter quantity can be evaluated efficiently.[9,10] Furthermore, each Gaussian state $\Psi = |\mathbf{q}_0; \tau\rangle$ has a well-defined configuration that can be visualized naturally by associating the positions of the particles with $\mathbf{q}_\tau$. At least this circumstance makes the VGW method more attractive than alternative approaches, for example, based on path integrals, in which the ground state wave function is not available explicitly, and so its visualization may not be straightforward, even in the cases when the wave function is localized. This is due to the difficulty associated with the choice of an unambiguous coordinate frame for a cluster.

Two forms of VGW exist, the fully coupled (FC-VGW) in which $\mathbf{G}$ is a full $3n \times 3n$ matrix that incorporates all the interparticle couplings, and the single particle form (SP-VGW), in which $\mathbf{G}$ is block diagonal, consisting of n blocks, each having size 3×3. (For a general harmonic potential

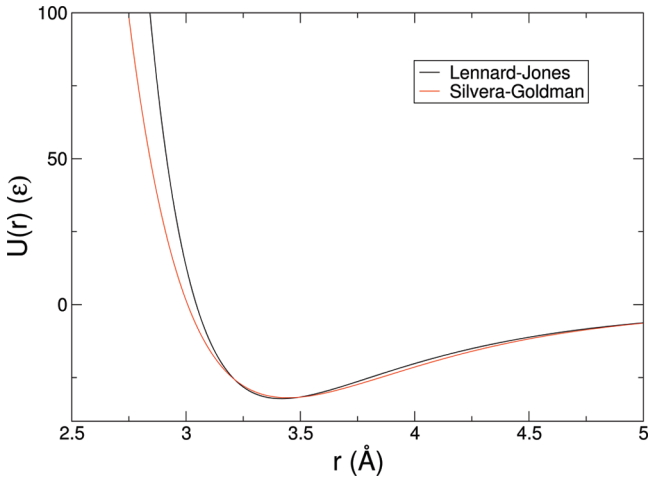

Figure 1. Lennard-Jones pair potential with $\sigma = 3.045$ Å and $\varepsilon = 32.25\ k_B K$ overlaid with the SG Goldman potential for p-H_2.

TABLE 1: Parameters of the Gaussians (cf. Equation 9) Used to Approximate the SG Potential

p	c_p ($k_B K$)	α_p (Å^{-2})
1	96 609.488 289 873	1.038 252 215 127
2	14 584.620 755 0751	0.597 403 910 9464
3	−365.460 614 956 589	0.196 476 572 277 834
4	−19.553 469 780 0036	0.066 686 117 717 81

only the FC-VGW is exact, while the SP-VGW is an approximation.)

For the present study, the intermolecular interactions for both p-H_2 and o-D_2 are represented by the Silvera−Goldman (SG) pair potential.[26] This potential can be fit by the LJ pair potential with $\varepsilon = 32.25$ K and $\sigma = 3.045$ Å. As can be seen from Figure 1 the two potentials are quite similar, especially near the minimum. This allows us to relate the present results with those obtained previously for the monatomic LJ clusters.[13] Using this LJ fit, the corresponding value of the de Boer quantum delocalization parameter[14] for p-H_2 is $\Lambda_{H_2} = 0.284$ and for o-D_2, $\Lambda_{D_2} = 0.201$. We also note that a fit similar to the present LJ-fit to the SG potential was used in ref 22, whereas another LJ potential has been used in ref 21. However, the latter potential deviates significantly from the above specified LJ potential.

The VGW eqs 5 are solved most efficiently when the pair potential is represented by a sum of Gaussians,

$$V(r_{ij}) \approx \sum_{p=1}^{P} c_p \exp(-\alpha_p r_{ij}^2) \tag{9}$$

We used the four-term fit of ref 27 with the parameters given in Table 1.

Ground State Estimation by Global Minimization of an Effective Potential Using GMIN

Consider the particle density:

$$\rho(\mathbf{q};\beta) := \langle \mathbf{q};0|e^{-\beta\hat{H}}|\mathbf{q};0\rangle \approx \langle \mathbf{q};\beta/2|\mathbf{q};\beta/2\rangle \tag{10}$$

where $|\mathbf{q};\beta/2\rangle$ is the VGW approximation to the solution of the Bloch eq (4). Now define the effective PES:

$$E(\mathbf{q};\beta) := -\frac{\partial \ln[\rho(\mathbf{q};\beta)]}{\partial\beta} \tag{11}$$

For any $\mathbf{q}$ the function $E(\mathbf{q};\beta)$ decreases monotonically with β. Moreover, using an argument based on the variational

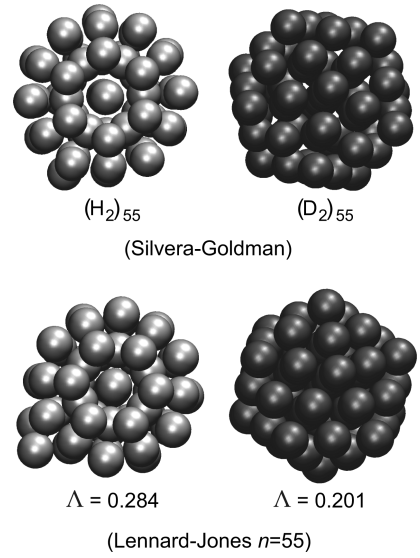

Figure 2. The ground state structures of LJ clusters with $n = 55$ (bottom) for quantum parameter pertaining to p-H_2 and o-D_2 found in ref 13 and those found in the present study with GMIN using the SG potential (top).

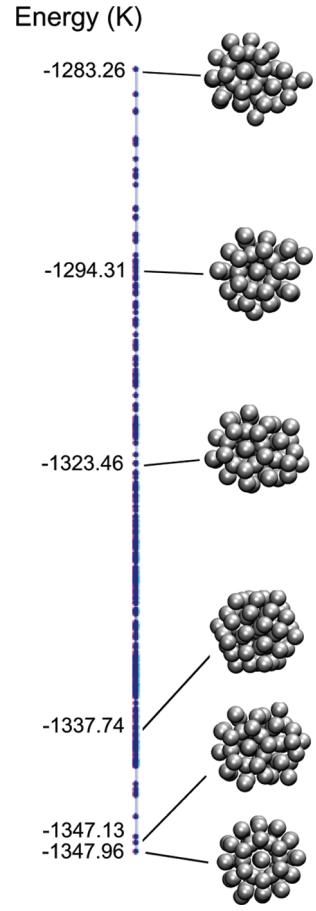

Figure 3. The 347 different low energy configurations found from the $(H_2)_{55}$ simulation, which occupy a relatively narrow energy range.

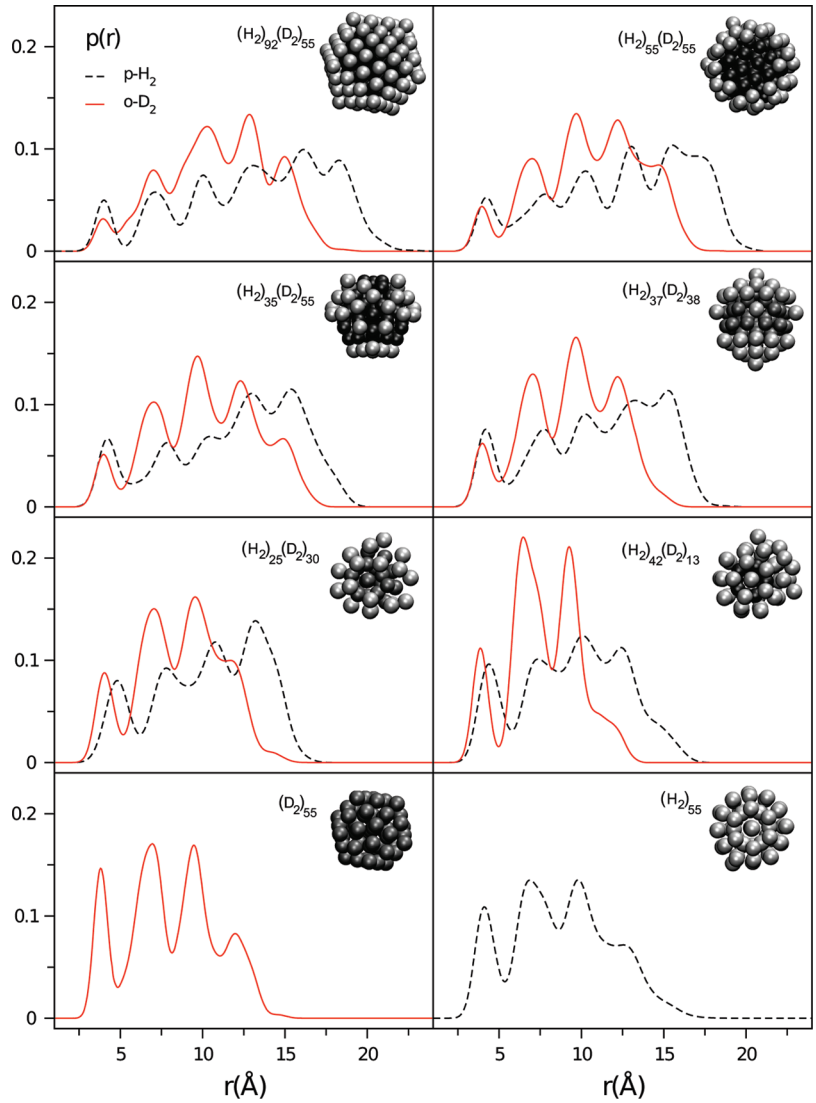

Figure 4. The radial pair correlation functions of the o-D_2 and p-H_2 components for several p-H_2/o-D_2 binary or homogeneous clusters. The corresponding cluster configurations are also shown with the dark spheres representing the o-D_2 molecules.

principle it gives an upper estimate for the true ground state energy

$$E(\mathbf{q};\beta) \geq E_0 \tag{12}$$

For a general potential, $E(\mathbf{q};\infty)$ provides the closest approximation to E_0 within the Gaussian ansatz (3), whereas for the special case of harmonic potential the form of eq 3 results in the exact ground state, $E(\mathbf{q};\infty) = E_0$.

Given an efficient numerical procedure of computing the effective PES $E(\mathbf{q};\beta)$, the problem of the ground state estimation with Hamiltonian $\hat{H}$ is recast naturally as the problem of global optimization of $E(\mathbf{q};\beta)$ for some sufficiently large value of β. Although this problem can be solved by any general global optimization algorithm, we note that at large β the function, $E(\mathbf{q};\beta)$, to be optimized is nearly piece-wise constant, that is,

$$\frac{\partial E(\mathbf{q};\beta)}{\partial \mathbf{q}} = 0 \quad (\beta \to \infty) \tag{13}$$

everywhere, except for the boundaries separating the basins of attraction, where it is discontinuous. This makes it suitable for minimization using the basin-hopping algorithm as utilized within GMIN.[5−7] The latter is designed for global optimization of the PES, $U(\mathbf{r})$, of a classical system. In the basin-hopping algorithm one minimizes the piecewise constant function $E(\mathbf{r})$, the value of which at a point $\mathbf{r}$ is set equal to the energy of the closest local minimum of the original PES $U(\mathbf{r})$.

Although $E(\mathbf{q};\beta)$ already has a favorable landscape, that is, the high barriers separating different local minima are minimized, the search for the global minimum can still be facilitated by an efficient sampling, such as that provided by the REMC method. Consequently, the REMC method was implemented here using, for a typical run, five random walks with temperatures in the range of 1−25 K. The quantum quenching (i.e., the Gaussian propagation) in this case was done with the less expensive SP-VGW version using the value of $\beta = 1.5\ (k_B K)^{-1}$. In addition to the standard REMC moves (i.e., a Metropolis local move and a configuration exchange between two replicas), for the case of binary systems, a move corresponding to an attempt of exchanging unlike molecules in a randomly chosen H_2−D_2 pair was also implemented. For each cluster we used approximately 10^6 MC moves per temperature. At least 100 distinct lowest energy (SP-VGW) configurations that emerged during the whole simulation period were collected. In the end of the simulation these configurations

were quenched again, but with the more accurate FC-VGW version and using $\beta = 5\ (k_B K)^{-1}$. The quenched (FC-VGW) configuration having the lowest energy $E(\mathbf{q};\beta)$ was then identified as a putative ground state configuration.

Results and Discussion

$(H_2)_{n-k}(D_2)_k$ binary clusters with compositions $(n, k) = (55, 13)$, $(55, 30)$, $(75, 38)$, $(90, 55)$, $(110, 55)$, and $(147, 55)$ were simulated. We used the following particle masses: $m_{H_2} = 2.016$ u and $m_{D_2} = 4.028$ u.

The cluster sizes and compositions were chosen to enable comparisons to our previous study of quantum LJ clusters[13] for the corresponding values of the quantum parameter ($\Lambda_{H_2} = 0.284$ and $\Lambda_{D_2} = 0.201$). It was demonstrated in ref 13 that the quantum delocalization leads to disordering of otherwise more symmetrical clusters. For example, the global minimum of classical LJ_{55} is complete Mackay icosahedron, as well as that of quantum $(D_2)_{55}$, but $(H_2)_{55}$ is predicted to possess a more disordered structure characterized by an anti-Mackay double-layer surrounding a 13-atom core. The corresponding configurations are shown in Figure 2. Also shown are the configurations obtained by GMIN in the present study using the SG potential. It can be observed that the $(D_2)_{55}$ configurations found in both potentials are identical, whereas the two $(H_2)_{55}$ configurations are slightly different, although they belong to the same structural motif.

Although we report the putative ground state configurations for the clusters herein, the results are at most a best estimate, as the number of local minima is too excessive, even for homogeneous clusters. To illustrate this, in Figure 3 the energies of the several hundred low energy configurations found from a particular simulation of $(H_2)_{55}$ using 10^6 MC steps are depicted. These configurations occupy a relatively narrow energy range. As discussed, the number of possible local minima for the mixed clusters can be many orders of magnitude greater, which leads to an increased sampling difficulty.

Figure 4 shows the putative ground state configurations for several clusters considered in this study. The predominant trend observed in all cases is the migration of the o-D_2 molecules to the center of the cluster. This confirms the earlier predictions by Chakravarty[17] followed by some recent studies,[19,20] both using PIMC based methods.

Also shown in Figure 4 are the radial pair correlation functions $p(r)$ for each of the two components, one reflecting the symmetric arrangement of the o-D_2 molecules in the Mackay icosahedral core of the cluster, and the other is the disordered arrangement of the p-H_2 molecules in the anti-Mackay overlayer.

All the ground state configurations found in the present study have the same general structure as that predicted in ref 13 for the homogeneous clusters of p-H_2 and o-D_2, where both of the latter share the same structural motifs for all sizes herein except $n = 55$. The ground state structures found for the binary $n = 55$ clusters belong to the disordered motif of the pure p-H_2 (being nearly identical), and we observe no shift to more ordered configurations when we increase the number of o-D_2 constituents, as, for example, in $(H_2)_{25}(D_2)_{30}$. Also, we observe no ordering/disordering effects caused by replacing a few p-H_2 molecules by o-D_2 molecules.

In conclusion, a method of estimating the ground state energy and structure of a weakly quantum many-body system has been presented. The method utilizes the fact that the ground state wave function is localized and as such can be well approximated by a VGW. The variational problem of finding the lowest-energy VGW was then reformulated as a problem of finding the global minimum of an effective PES. The method has been incorporated into GMIN and demonstrated on several binary *para*-hydrogen/*ortho*-deuterium clusters. The method is conceptually simple and numerically efficient and allows one to visualize the quantum ground state wave functions by assigning a position vector to each particle.

Acknowledgment. This work was supported by the NSF grant CHE-0809108. We thank David Wales for his generous help with incorporation of the VGW algorithm into GMIN.

References and Notes

(1) Marques, J. M. C.; Periera, F. B. *Chem. Phys. Lett.* **2010**, *485*, 211.
(2) Leary, R. H. *J. Global Optimization* **1997**, *11*, 35.
(3) Stillinger, F. H.; Weber, T. A. *Phys. Rev. A* **1983**, *28*, 2408. (a) Tsai, C. J.; Jordan, K. D. *J. Phys. Chem.* **1993**, *97*, 11227. (b) Stillinger, F. H. *Phys. Rev. E* **1999**, *59*, 48.
(4) Geyer, C. J. In *Computing Science and Statistics: Proceedings of the 23rd Symposium on the Interface*; Keramigas, E. M., Ed.; Interface Foundation: Fairfax, 1991; pp 156−163; Hukushima, K.; Nemoto, K. *J. Phys. Soc. Jpn.* **1996**, *65*, 1604.
(5) Wales, D. J.; Doye, J. P. K. *J. Phys. Chem. A* **1997**, *101*, 5111.
(6) Bogdan, T. V.; Wales, D. J.; Calvo, F. *J. Chem. Phys.* **2006**, *124*, 044102.
(7) http://www-wales.ch.cam.ac.uk/GMIN/.
(8) Predescu, C.; Sabo, D.; Doll, J. D.; Freeman, D. L. *J. Chem. Phys.* **2003**, *119*, 12119. (a) Sabo, D.; Predescu, C.; Doll, J. D.; Freeman, D. L. *J. Chem. Phys.* **2004**, *121*, 856.
(9) Frantsuzov, P.; Mandelshtam, V. A. *J. Chem. Phys.* **2004**, *121*, 9247.
(10) Predescu, C.; Frantsuzov, P. A.; Mandelshtam, V. A. *J. Chem. Phys.* **2005**, *122*, 154305.
(11) Doye, J. P. K.; Calvo, F. *J. Chem. Phys.* **2002**, *116*, 8307.
(12) Calvo, F.; Doye, J. P. K.; Wales, D. J. *J. Chem. Phys.* **2001**, *114*, 7312.
(13) Deckman, J.; Mandelshtam, V. A. *J. Phys. Chem. A* **2009**, *113*, 7394.
(14) de Boer, J. *Physica (Amdsterdam)* **1948**, *14*, 139.
(15) Sindzingre, P.; Ceperley, D.; Klein, M. *Phys. Rev. Lett.* **1991**, *67*, 1871.
(16) Scharf, D.; Martyna, G.; Klein, M. *Chem. Phys. Lett.* **1992**, *197*, 231.
(17) Chakravarty, C. *Phys. Rev. Lett.* **1995**, *75*, 1727.
(18) Chakravarty, C. *J. Chem. Phys.* **2002**, *116*, 8938.
(19) Mezzacapo, F.; Boninsegni, M. *Phys. Rev. A* **2007**, *76*, 021201.
(20) Cuervo, J. E.; Roy, P. N. *J. Chem. Phys.* **2009**, *131*, 114302.
(21) Mezzacapo, F.; Boninsegni, M. *J. Physics: Conf. Ser.* **2009**, *150*, 032059.
(22) Warnecke, S.; Sevryuk, M. B.; Ceperley, D. M.; Toennies, J. P.; Guardiola, R.; Navarro, J. *Eur. Phys. J. D* **2010**, *56*, 353.
(23) Clarke, A. S.; Kapral, R.; Moore, B.; Patey, G.; Wu, X.-G. *Phys. Rev. Lett.* **1993**, *70*, 3283.
(24) Clarke, A. S.; Kapral, R.; Patey, G. N. *J. Chem. Phys.* **1994**, *101*, 2432.
(25) Doye, J.; Meyer, L. *Phys. Rev. Lett.* **2005**, *95*, 063401.
(26) Silvera, I. F.; Goldman, V. V. *J. Chem. Phys.* **1978**, *69*, 4209.
(27) Poulsen, J. A.; Nyman, G.; Rossky, P. J, *J. Phys. Chem.* **2004**, *108*, 19799.

JP102898B